PERGAMON

International Journal of Solids and Structures 39 (2002) 2871–2892

INTERNATIONAL JOURNAL OF SOLIDS and STRUCTURES

www.elsevier.com/locate/ijsolstr

Two- and three-dimensional transient thermoelastic analysis by BEM via particular integrals

K.-H. Park, P.K. Banerjee *

Department of Civil Engineering, State University of New York at Buffalo, 240 Ketter Hall, 14260 Amherst, Buffalo, NY 14260, USA

Abstract

Particular integral formulations are presented for two- and three-dimensional transient uncoupled thermoelastic analysis. These formulations differ from previous particular integral formulations in that the equation of uncoupled thermoelasticity including the heat conduction equation is fully satisfied to obtain particular integrals. The equation of the steady-state thermoelasticity is now used as the complementary solution and two global shape functions are considered to approximate the transient term of the heat conduction equation so that two sets of particular integrals could be derived.

The numerical results for both sets of particular integrals are given for three example problems and compared with their analytical solutions.

Keywords: Boundary element method; Thermoelasticity; Particular integrals; Heat transfer; Computational mechanics

1. Introduction

Boundary element methods (BEM) have been developed into a powerful numerical method for solving transient thermoelastic problems. The direct application of the BEM to the transient thermoelastic problems generates a domain integral in addition to the usual surface integrals (Banerjee, 1994). Generally three methods have been proposed over the years to eliminate this volume integration problem: (1) the convolution method, (2) the volume integral conversion method and (3) the particular integral method.

Over the last 20 years the convolution method, using the time-domain fundamental solution and a time-stepping technique, has been fully developed for multi-region axisymmetric, two- (2D) and three-dimensional (3D) thermoelasticity as well as thermoplasticity (Dargush, 1987; Dargush and Banerjee, 1989, 1990, 1991a, 1991b, 1992; Chopra, 1992; Wang, 1995). While the convolution method gives excellent results, this approach suffers from the need to store the entire displacement, stress and temperature history of the solution to evaluate the convolution integrals, which requires a substantial amount of computer resources. Therefore a more practical alternative must be developed.

* Corresponding author. Tel.: +1-716-645-2114; fax: +1-716-645-3945.
E-mail address: pkb@eng.buffalo.edu (P.K. Banerjee).

0020-7683/02/$ - see front matter
PII: S0020-7683(02)00125-7

Another alternative is the volume integral conversion method which transforms exactly the volume integral into integrals over the boundary. The exact form of volume integral conversion method for 3D thermoelasticity was presented by Rizzo and Shippy (1977). Later, Banerjee and Butterfield (1981) and Banerjee (1994) also described the exact form for both 2D and 3D stress analyses of bodies subjected to a distribution of temperature or a hydraulic potential. While these are boundary-only formulations, their approach lacked generality and was restricted essentially to steady-state temperature distributions. Although it is now possible to convert the volume integrals into a boundary integral form using global shape function (GSF) for the time derivative term, this approach has not been investigated here (for details see Park (2001)).

The other alternative is the particular integral method that obtains a total solution as the sum of a complementary solution for the governing homogeneous differential equation and a particular solution for the governing inhomogeneous differential equation. Henry and Banerjee (1988) first developed the particular integral formulations for 2D and 3D transient uncoupled thermoelasticity by adopting a body force point-of-view for the thermal loading. Subsequently, Deb and Banerjee (1991) used a multiple regression scheme for the known temperature data to derive the particular integrals for the exact representation of temperature distributions up to the quadratic order in both two and three dimensions. Particular integrals for the uncoupled quasistatic thermoelastic analysis of an anisotropic medium were presented by Deb et al. (1991). Recently, Raveendra (2000) presented the particular integral formulations for axisymmetric uncoupled thermoelastic analysis by using piecewise polynomial basis functions. However, all of the previous formulations (mentioned above) for thermoelastic analysis were developed by using only the Navier equation with the known temperature data, without considering the heat conduction equation.

In order to eliminate the need for the known temperature data as input, as in the previous formulations, a new particular integral formulation for 2D and 3D transient thermoelastic analysis is presented by developing solutions of the uncoupled thermoelasticity equation including the equation of heat conduction. The solution of the equation of the steady-state uncoupled thermoelasticity is used as the complementary function. The particular integrals for displacement, traction, temperature and flux are derived by using two GSFs, GSF1—$(R-r)$ and GSF2—$(R^2-r^2\ln r)$. In this newly developed analysis the unknown displacement and traction can be obtained together with the unknown temperature and flux in a single analysis. In order to evaluate the accuracy of the present formulations, results obtained for three example problems are compared with their analytical solutions (AS). The effects of aspect ratios of a region and inclusion of interior points are also discussed.

2. Previous particular integral formulation

In order to appreciate the essential features of the present formulation, the previous particular integral formulation developed by Henry and Banerjee (1988) is first briefly examined here.

The governing differential equation of uncoupled thermoelasticity used in the previous formulation is the Navier equation, which is expressed in terms of displacement u_i as

$$(\lambda+\mu)u_{j,ji}+\mu u_{i,jj}=(3\lambda+2\mu)\alpha T_{,i} \tag{1}$$

where λ and μ are Lame's constants, α is the thermal coefficient of expansion, commas represent differentiation with respect to spatial coordinates, and $i, j = 1, 2(3)$ for two(three) dimensions.

The solution of the above equation can be represented as a sum of complementary function u_i^c satisfying the homogeneous equation

$$(\lambda+\mu)u^c_{j,ji}+\mu u^c_{i,jj}=0 \tag{2}$$

and particular integral u_i^{p} satisfying the inhomogeneous equation

$$(\lambda+\mu)u^{\mathrm{p}}_{j,ji}+\mu u^{\mathrm{p}}_{i,jj}=(3\lambda+2\mu)\alpha T_{,i} \tag{3}$$

Then the total solutions for displacement u_i and traction t_i can be expressed as

$$u_i=u_i^{\mathrm{c}}+u_i^{\mathrm{p}} \tag{4a}$$

$$t_i=t_i^{\mathrm{c}}+t_i^{\mathrm{p}} \tag{4b}$$

where t_i^{c} and t_i^{p} are the complementary function and particular integral for traction respectively.

It should be noted here that the homogeneous Eq. (2) is that of the ordinary elastostatics.

By using Goodier's method (Timoshenko and Goodier, 1951), the particular integral for displacement can be expressed as a gradient of a thermoelastic displacement potential $h(\mathbf{x})$

$$u_i^{\mathrm{p}}(\mathbf{x})=h_{,i}(\mathbf{x}) \tag{5}$$

Substituting of Eq. (5) into Eq. (3) yields

$$h_{,jj}(\mathbf{x})=\gamma T(\mathbf{x}) \tag{6}$$

where

$$\gamma=\frac{(3\lambda+2\mu)\alpha}{(\lambda+2\mu)}.$$

By introducing the concept of GSF $C(\mathbf{x},\xi_n)$, the unknown temperature $T(\mathbf{x})$ can be approximated as

$$T(\mathbf{x})=\sum_{n=1}^{\infty}C(\mathbf{x},\xi_n)\phi(\xi_n) \tag{7}$$

where $\phi(\xi_n)$ is a set of fictitious scalar densities.

Then the thermoelastic displacement potential $h(\mathbf{x})$ and the particular integrals for displacement u_i^{p}, stress σ_i^{p}, and traction t_i^{p} can be found as (Henry and Banerjee, 1988)

$$h(\mathbf{x})=\sum_{n=1}^{\infty}K(\mathbf{x},\xi_n)\phi(\xi_n) \tag{8}$$

$$u_i^{\mathrm{p}}(\mathbf{x})=\sum_{n=1}^{\infty}U_i(\mathbf{x},\xi_n)\phi(\xi_n) \tag{9}$$

$$\sigma_{ij}^{\mathrm{p}}(\mathbf{x})=\sum_{n=1}^{\infty}S_{ij}(\mathbf{x},\xi_n)\phi(\xi_n) \tag{10}$$

$$t_i^{\mathrm{p}}(\mathbf{x})=\sum_{n=1}^{\infty}H_i(\mathbf{x},\xi_n)\phi(\xi_n) \tag{11}$$

where

$$S_{ij}(\mathbf{x},\xi_n)=\delta_{ij}\lambda E_{ll}+2\mu E_{ij}-\delta_{ij}(3\lambda+2\mu)\alpha C$$

$$H_i(\mathbf{x},\xi_n)=S_{ij}(\mathbf{x},\xi_n)n_j(\mathbf{x})$$

and

$n_j(\mathbf{x})=$ unit normal at x in the jth direction.

Table 1
Comparison of functions in two formulations

Function	Previous	Present
$C(\mathbf{x}, \xi_n)$	$R - r$	$R - r$
$D(\mathbf{x}, \xi_n)$	–	$(C_1R - C_2r)r^2$
$K(\mathbf{x}, \xi_n)$	$(B_1R - B_2r)r^2$	–
$U_i(\mathbf{x}, \xi_n)$	$(2B_1R - 3B_2r)y_i$	$(D_1R - D_2r)r^2y_i$
$E_{ij}(\mathbf{x}, \xi_n)$	$(2B_1R - 3B_2r)\delta_{ij} - 3B_2y_iy_j/r$	$(D_1R - D_2r)r^2\delta_{ij} + (2D_1R - 3D_2r)y_1y_j$
$S_{ij}(\mathbf{x}, \xi_n)$	$\delta_{ij}\lambda E_{ll} + 2\mu E_{ij} - \delta_{ij}(3\lambda + 2\mu)\alpha C$	$\delta_{ij}\lambda E_{ll} + 2\mu E_{ij} - \delta_{ij}(3\lambda + 2\mu)\alpha D$

Note: $B_1 = \gamma/2d$, $B_2 = \gamma/(3(1 + d))$, $\gamma = (3\lambda + 2\mu)\alpha/(\lambda + 2\mu)$.

Functions C, K, U_i, E_{ij}, and S_{ij} in the above equations are summarized in Table 1 for the purposes of comparison with those of the present formulation.

Finally one can obtain the following numerical implementation in matrix form (Henry and Banerjee, 1988)

$$[G]\{t\} - [F]\{u\} = [M]\{T\} \tag{12}$$

where

$$[M] = \{[G][H] - [F][U]\}[C]^{-1} \tag{13}$$

It should be noted from Eq. (12) that the unknown displacement or traction can be obtained with the known temperature as input data, which must be determined from a separate analysis.

3. New particular integral formulation

Unlike the previous formulation, the governing differential equation of uncoupled thermoelasticity used for the present formulation includes the heat conduction equation in addition to the Navier equation,

$$(\lambda + \mu)u_{j,ji} + \mu u_{i,jj} - (3\lambda + 2\mu)\alpha T_{,i} = 0 \tag{14}$$

$$kT_{,jj} - \rho c_\varepsilon \dot{T} = 0 \tag{15}$$

where k is the conductivity, ρ the mass density, c_ε the specific heat at constant strain, and a superposed dot denotes a time derivative.

The solution of the above equations can be represented as a sum of complementary functions u_i^{c} and T^{c} satisfying the homogeneous equations

$$(\lambda + \mu)u^{\mathrm{c}}_{j,ji} + \mu u^{\mathrm{c}}_{i,jj} - (3\lambda + 2\mu)\alpha T^{\mathrm{c}}_{,i} = 0 \tag{16}$$

$$kT^{\mathrm{c}}_{,jj} = 0 \tag{17}$$

and particular integrals u_i^{p} and T^{p} satisfying the total inhomogeneous equations

$$(\lambda + \mu)u^{\mathrm{p}}_{j,ji} + \mu u^{\mathrm{p}}_{i,jj} - (3\lambda + 2\mu)\alpha T^{\mathrm{p}}_{,i} = 0 \tag{18}$$

$$kT^{\mathrm{p}}_{,jj} - \rho c_\varepsilon \dot{T} = 0 \tag{19}$$

It should be noted that the homogeneous Eqs. (16) and (17) now are those for the steady-state thermoelasticity.

3.1. Complementary solutions

The boundary integral equation of the homogeneous differential Eqs. (16) and (17) can be expressed as (Dargush and Banerjee, 1991a; Banerjee, 1994)

$$\begin{Bmatrix} C_{ij} & u_i^{\mathrm{c}}(\xi) \\ C_T & T^{\mathrm{c}}(\xi) \end{Bmatrix} = \int \left(\begin{bmatrix} G_{ij} & G_{jT} \\ 0 & G_{TT} \end{bmatrix} \begin{Bmatrix} t_i^{\mathrm{c}}(\mathbf{x}) \\ q^{\mathrm{c}}(\mathbf{x}) \end{Bmatrix} - \begin{bmatrix} F_{ij} & F_{jT} \\ 0 & F_{TT} \end{bmatrix} \begin{Bmatrix} u_i^{\mathrm{c}}(\mathbf{x}) \\ T^{\mathrm{c}}(\mathbf{x}) \end{Bmatrix} \right) \mathrm{d}S(\mathbf{x}) \tag{20}$$

where q^{c} is the complementary function for flux, the coefficients C_{ij} and C_T represent the jump terms resulting from the singular nature of F_{ij} and F_{TT} respectively, and G_{ij}, G_{jT}, G_{TT}, F_{ij}, F_{jT} and F_{TT} are defined in the Appendix A.

The total solutions for displacement u_i, traction t_i, temperature T and flux q are

$$u_i = u_i^{\mathrm{c}} + u_i^{\mathrm{p}} \tag{21a}$$

$$t_i = t_i^{\mathrm{c}} + t_i^{\mathrm{p}} \tag{21b}$$

$$T = T^{\mathrm{c}} + T^{\mathrm{p}} \tag{21c}$$

$$q = q^{\mathrm{c}} + q^{\mathrm{p}} \tag{21d}$$

where q^{p} is the particular integral for flux.

3.2. Particular integrals

Eq. (19) contains the time derivative of unknown transient temperature $\dot{T}(\mathbf{x})$ within domain. By assuming the function can be represented by an infinite series, an expression relating $\dot{T}(\mathbf{x})$ to a set of fictitious scalar densities $\dot{\phi}(\xi_n)$ via a GSF $C(\mathbf{x}, \xi_n)$ can be written as

$$\dot{T}(\mathbf{x}) = \sum_{n=1}^{\infty} C(\mathbf{x}, \xi_n) \dot{\phi}(\xi_n) \tag{22}$$

Since the GSF is used to approximate $\dot{T}(\mathbf{x})$, the choice of these functions has direct effects on the accuracy of this method. Several functions were considered and two functions are chosen for illustration:

$$\text{GSF1:}\ \ C(\mathbf{x}, \xi_n) = R - r \tag{23a}$$

$$\text{GSF2:}\ \ C(\mathbf{x}, \xi_n) = R^2 - r^2 \ln r \tag{23b}$$

where r is the distance between $\mathbf{x}$ and ξ_n, and R is a constant chosen to be the largest dimension of the problem domain.

Then the particular integrals which satisfy Eqs. (18) and (19) can be found as (see Appendix B)

$$T^{\mathrm{p}}(\mathbf{x}) = \sum_{n=1}^{\infty} D(\mathbf{x}, \xi_n) \dot{\phi}(\xi_n) \tag{24}$$

$$u_i^{\mathrm{p}}(\mathbf{x}) = \sum_{n=1}^{\infty} U_i(\mathbf{x}, \xi_n) \dot{\phi}(\xi_n) \tag{25}$$

where

$$D(\mathbf{x},\xi_n) = (C_1 R - C_2 r)r^2 \quad \text{for GSF1} \tag{26a}$$

$$= \left(C_1' R^2 - C_2' r^2 - C_3' r^2 \ln r\right) r^2 \quad \text{for GSF2} \tag{26b}$$

$$U_i(\mathbf{x},\xi_n) = (D_1 R - D_2 r)r^2 y_i \quad \text{for GSF1} \tag{27a}$$

$$= \left(D_1' R^2 - D_2' r^2 - D_3' r^2 \ln r\right) r^2 y_i \quad \text{for GSF2} \tag{27b}$$

$$C_1 = \frac{\kappa}{2d}; \quad C_2 = \frac{\kappa}{3(1+d)}; \quad C_1' = \frac{\kappa}{2d}; \quad C_2' = -\frac{(6+d)\kappa}{16(2+d)^2}; \quad C_3' = \frac{\kappa}{4(2+d)}$$

$$D_1 = \frac{\beta}{2d(2+d)}; \quad D_2 = \frac{\beta}{3(1+d)(3+d)};$$

$$D_1' = \frac{\beta}{2d(2+d)}; \quad D_2' = -\frac{\beta(d^2+14d+32)}{16(2+d)^2(4+d)^2}; \quad D_3' = \frac{\beta}{4(2+d)(4+d)}$$

$\kappa = \rho c_\varepsilon / k$, $\beta = \kappa\alpha(3\lambda + 2\mu)/(\lambda + 2\mu)$, and d is the dimensionality of the problem.

A particular integral for stress can be derived by substituting Eqs. (24) and (25) into the strain–displacement relation and the stress–strain law:

$$\sigma_{ij}^{\mathrm{p}}(\mathbf{x}) = \sum_{n=1}^{\infty} S_{ij}(\mathbf{x},\xi_n)\dot{\phi}(\xi_n) \tag{28}$$

where

$$S_{ij}(\mathbf{x},\xi_n) = \delta_{ij}\lambda E_{ll} + 2\mu E_{ij} - \delta_{ij}(3\lambda + 2\mu)\alpha D \tag{29}$$

$$E_{ll}(\mathbf{x},\xi_n) = \{(2+d)D_1 R - (3+d)D_2 r\} r^2 \quad \text{for GSF1} \tag{30a}$$

$$= \left\{(2+d)D_1' R^2 - \left\{(4+d)D_2' + D_3'\right\} r^2 - 4(4+d)D_3' r^2 \ln r\right\} r^2 \quad \text{for GSF2} \tag{30b}$$

$$E_{ij}(\mathbf{x},\xi_n) = (D_1 R - D_2 r)r^2 \delta_{ij} + (2D_1 R - 3D_2 r) y_i y_j \quad \text{for GSF1} \tag{31a}$$

$$= \left(D_1' R^2 - D_2' r^2 - D_3' r^2 \ln r\right) r^2 \delta_{ij} + \left\{2D_1' R^2 - (4D_2' + D_3') r^2 - 4D_3' r^2 \ln r\right\} y_i y_j \quad \text{for GSF2} \tag{31b}$$

Then a particular integral for traction is derived by multiplying the above equation with appropriate normals:

$$t_i^{\mathrm{p}}(\mathbf{x}) = \sum_{n=1}^{\infty} H_i(\mathbf{x},\xi_n)\dot{\phi}(\xi_n) \tag{32}$$

where

$$H_i(\mathbf{x},\xi_n) = S_{ij}(\mathbf{x},\xi_n) n_j(\mathbf{x})$$

A particular integral for flux can be then derived from Eq. (24) as

$$q^{\mathrm{p}}(\mathbf{x}) = \sum_{n=1}^{\infty} Q(\mathbf{x},\xi_n)\dot{\phi}(\xi_n) \tag{33}$$

where

$$Q(\mathbf{x},\xi_n) = -k\frac{\partial D}{\partial n} = -k(2C_1R - 3C_2r)y_in_i \quad \text{for GSF1} \tag{34a}$$

$$= -k\left(2C_1'R^2 - (4C_2' + C_3')r^2 - 4C_3'r^2\ln r\right)y_in_i \quad \text{for GSF2} \tag{34b}$$

The details of derivation for particular integrals u_i^{p}, t_i^{p}, T^{p} and q^{p} using the global shape function GSF1 are given in Appendix B. The particular integrals using the global shape function GSF2 can be derived in the same manner as shown in Appendix B. It is very clear from Table 1 that the particular integrals, which are obtained by purely satisfying the Navier equation of elasticity with an arbitrary known temperature distribution, are quite different from those obtained by satisfying both heat and elasticity equations.

4. Numerical implementations

The boundary integral Eq. (20) for the steady-state thermoelasticity can be expressed in matrix form as (Banerjee, 1994)

$$\begin{bmatrix} G_{ij} & G_{jT} \\ 0 & G_{TT} \end{bmatrix}\begin{Bmatrix} t_i^{\mathrm{c}} \\ q^{\mathrm{c}} \end{Bmatrix} - \begin{bmatrix} F_{ij} & F_{jT} \\ 0 & F_{TT} \end{bmatrix}\begin{Bmatrix} u_i^{\mathrm{c}} \\ T^{\mathrm{c}} \end{Bmatrix} = 0 \tag{35}$$

Introducing Eqs. (21a)–(21d) in the above equation, the complementary functions are eliminated:

$$\begin{bmatrix} G_{ij} & G_{jT} \\ 0 & G_{TT} \end{bmatrix}\begin{Bmatrix} t_i \\ q \end{Bmatrix} - \begin{bmatrix} F_{ij} & F_{jT} \\ 0 & F_{TT} \end{bmatrix}\begin{Bmatrix} u_i \\ T \end{Bmatrix} = \begin{bmatrix} G_{ij} & G_{jT} \\ 0 & G_{TT} \end{bmatrix}\begin{Bmatrix} t_i^{\mathrm{p}} \\ q^{\mathrm{p}} \end{Bmatrix} - \begin{bmatrix} F_{ij} & F_{jT} \\ 0 & F_{TT} \end{bmatrix}\begin{Bmatrix} u_i^{\mathrm{p}} \\ T^{\mathrm{p}} \end{Bmatrix} \tag{36}$$

If a finite number of ξ_n, N, are chosen, the particular integrals for displacement, traction, temperature and flux can be written as

$$\begin{Bmatrix} u_i^{\mathrm{p}} \\ T^{\mathrm{p}} \end{Bmatrix} = \begin{bmatrix} U_i \\ D \end{bmatrix}\left\{\dot{\phi}\right\} \tag{37}$$

$$\begin{Bmatrix} t_i^{\mathrm{p}} \\ q^{\mathrm{p}} \end{Bmatrix} = \begin{bmatrix} H_i \\ Q \end{bmatrix}\left\{\dot{\phi}\right\} \tag{38}$$

Substituting Eqs. (37) and (38) into Eq. (36) and considering the fictitious nodal values as

$$\left\{\dot{\phi}\right\} = [C]^{-1}\left\{\dot{T}\right\} \tag{39}$$

one can obtain the following equation

$$\begin{bmatrix} G_{ij} & G_{jT} \\ 0 & G_{TT} \end{bmatrix}\begin{Bmatrix} t_i \\ q \end{Bmatrix} - \begin{bmatrix} F_{ij} & F_{jT} \\ 0 & F_{TT} \end{bmatrix}\begin{Bmatrix} u_i \\ T \end{Bmatrix} = \begin{bmatrix} M_{jT} \\ M_{TT} \end{bmatrix}\left\{\dot{T}\right\} \tag{40}$$

where

$$\begin{bmatrix} M_{jT} \\ M_{TT} \end{bmatrix} = \left\{\begin{bmatrix} G_{ij} & G_{jT} \\ 0 & G_{TT} \end{bmatrix}\begin{bmatrix} H_i \\ Q \end{bmatrix} - \begin{bmatrix} F_{ij} & F_{jT} \\ 0 & F_{TT} \end{bmatrix}\begin{bmatrix} U_i \\ D \end{bmatrix}\right\}[C]^{-1} \tag{41}$$

Using an explicit time integration scheme, Eq. (40) can be expressed as

$$\begin{bmatrix} G_{ij} & G_{jT} \\ 0 & G_{TT} \end{bmatrix}\begin{Bmatrix} t_i \\ q \end{Bmatrix}^t - \begin{bmatrix} F_{ij} & F_{jT} + \frac{1}{\Delta t}M_{jT} \\ 0 & F_{TT} + \frac{1}{\Delta t}M_{TT} \end{bmatrix}\begin{Bmatrix} u_i \\ T \end{Bmatrix}^t = -\frac{1}{\Delta t}\begin{bmatrix} M_{jT} \\ M_{TT} \end{bmatrix}\{T\}^{t-\Delta t} \tag{42}$$

The right side of Eq. (42) is known at time t, since it involves values that have been specified either as initial conditions or calculated previously. Introducing the boundary conditions at time t, the final system can be written as

$$[A]\{X\} = \{b\} \tag{43}$$

where X is unknown vector of displacement, traction, temperature and flux, b is a known vector and A is the coefficient matrix. Therefore the unknown displacement or traction can be obtained together with the unknown temperature or flux.

As mentioned in the previous works (Henry and Banerjee, 1988; Wang and Banerjee, 1988) the use of interior points usually leads to a better representation of the particular integrals. If the interior points are used, then formulation is modified as follows:

For convenience, define, for example,

$$\begin{aligned} \{u_\alpha\} &= \{u_1\ u_2\ T\}^{\mathrm{T}} \\ \{t_\alpha\} &= \{t_1\ t_2\ q\}^{\mathrm{T}} \end{aligned} \tag{44}$$

Utilizing this new convention Eq. (20) can be written for interior points as

$$\left\{u_\alpha^{\mathrm{c}}\right\}_{\mathrm{i}} = [G_{\beta\alpha}]_{\mathrm{i}}\left\{t_\beta^{\mathrm{c}}\right\}_{\mathrm{b}} - [F_{\beta\alpha}]_{\mathrm{i}}\left\{u_\beta^{\mathrm{c}}\right\}_{\mathrm{b}} \tag{45}$$

where subscript "i" denotes interior values and subscript "b" boundary values.

Substituting the total solutions, it can be rewritten as

$$[G_{\beta\alpha}]_{\mathrm{i}}\{t_\beta\}_{\mathrm{b}} - [F_{\beta\alpha}]_{\mathrm{i}}\{u_\beta\}_{\mathrm{b}} - \{u_\alpha\}_{\mathrm{i}} = [G_{\beta\alpha}]_{\mathrm{i}}\left\{t_\beta^{\mathrm{p}}\right\}_{\mathrm{b}} - [F_{\beta\alpha}]_{\mathrm{i}}\left\{u_\beta^{\mathrm{p}}\right\}_{\mathrm{b}} - \left\{u_\alpha^{\mathrm{p}}\right\}_{\mathrm{i}} \tag{46}$$

Considering Eqs. (37) and (38) as

$$\begin{aligned} \left\{u_\alpha^{\mathrm{p}}\right\}_{\mathrm{i}} &= [U_\alpha]_{\mathrm{i}}\left\{\dot{\phi}\right\}_{\mathrm{b+i}} \\ \left\{u_\alpha^{\mathrm{p}}\right\}_{\mathrm{b}} &= [U_\alpha]_{\mathrm{b}}\left\{\dot{\phi}\right\}_{\mathrm{b+i}} \\ \left\{t_\alpha^{\mathrm{p}}\right\}_{\mathrm{b}} &= [H_\alpha]_{\mathrm{b}}\left\{\dot{\phi}\right\}_{\mathrm{b+i}} \end{aligned} \tag{47}$$

and substituting the above equation into Eq. (46), one can obtain a system of equation for the interior points

$$[G_{\beta\alpha}]_{\mathrm{i}}\{t_\beta\}_{\mathrm{b}} - [F_{\beta\alpha}]_{\mathrm{i}}\{u_\beta\}_{\mathrm{b}} - \{u_\alpha\}_{\mathrm{i}} = ([G_{\beta\alpha}]_{\mathrm{i}}[H_\beta]_{\mathrm{b}} - [F_{\beta\alpha}]_{\mathrm{i}}[U_\beta]_{\mathrm{b}} - [U_\alpha]_{\mathrm{i}})\left\{\dot{\phi}\right\}_{\mathrm{b+i}} \tag{48}$$

Also for boundary points,

$$[G_{\beta\alpha}]_{\mathrm{b}}\{t_\beta\}_{\mathrm{b}} - [F_{\beta\alpha}]_{\mathrm{b}}\{u_\beta\}_{\mathrm{b}} = ([G_{\beta\alpha}]_{\mathrm{b}}[H_\beta]_{\mathrm{b}} - [F_{\beta\alpha}]_{\mathrm{b}}[U_\alpha]_{\mathrm{b}})\left\{\dot{\phi}\right\}_{\mathrm{b+i}} \tag{49}$$

Combining the above two equations and using Eq. (39), one obtains

$$\begin{bmatrix} [G_{\beta\alpha}]_{\mathrm{b}} \\ [G_{\beta\alpha}]_{\mathrm{i}} \end{bmatrix}\{t_\beta\}_{\mathrm{b}} - \begin{bmatrix} [F_{\beta\alpha}]_{\mathrm{b}} & 0 \\ [F_{\beta\alpha}]_{\mathrm{i}} & I \end{bmatrix}\begin{Bmatrix} \{u_\beta\}_{\mathrm{b}} \\ \{u_\beta\}_{\mathrm{i}} \end{Bmatrix} = [M_\alpha]_{\mathrm{b+i}}\left\{\dot{T}\right\}_{\mathrm{b+i}} \tag{50}$$

where

$$[M_\alpha]_{\mathrm{b+i}} = \left(\begin{bmatrix} [G_{\beta\alpha}]_{\mathrm{b}} \\ [G_{\beta\alpha}]_{\mathrm{i}} \end{bmatrix}[H_\beta]_{\mathrm{b}} - \begin{bmatrix} [F_{\beta\alpha}]_{\mathrm{b}} \\ [F_{\beta\alpha}]_{\mathrm{i}} \end{bmatrix}[U_\beta]_{\mathrm{b}} - \begin{bmatrix} 0 \\ [U_\alpha]_{\mathrm{i}} \end{bmatrix}\right)[C]_{\mathrm{b+i}}^{-1} \tag{51}$$

and I is identity matrix.

By using the explicit time integration scheme and incorporating the known boundary conditions, the final system of equation can be then cast into the same form as in Eq. (43).

5. Numerical examples

In order to test the accuracy of the present formulations, three example problems are solved and the results are compared with the AS. The first example is presented to demonstrate the effects of the aspect ratio and inclusion of interior points. For second and third examples 3D applications of the present formulations are described for the two GSFs. The material properties used in all these example problems are: $E = 1.0$, $\alpha = 0.02$, $v = 0.3$, $k = 1.0$ and $\rho c_\varepsilon = 1.0$ and all state variables are assumed to be zero initially.

5.1. Example 1: a unit cube

The first example is a unit cube that is initially at zero temperature and is subjected to a sudden heat on one of its faces. The cube assumes to be in plane strain with three of its four lateral sides insulated and restrained from normal displacement. The heated face is raised and maintained at a temperature of unity (Fig. 1). Additionally for the 3D idealization the front and back faces are assumed to be insulated with roller supports.

The AS of temperature T, displacement u and lateral stress σ_x for this example problem can be found in the classical books of Carslaw and Jaeger (1959, p. 100) and Timoshenko and Goodier (1951, p. 401) as

$$T(y,t) = 1 - \frac{4}{\pi}\sum_{n=0}^{\infty}\frac{(-1)^n}{2n+1}\exp\left(-\frac{(2n+1)^2\pi^2\kappa t}{4L^2}\right)\cos\left(\frac{(2n+1)\pi y}{2L}\right)$$

$$u(y,t) = \frac{(1+v)\alpha}{(1-v)}\int_0^y T\,\mathrm{d}y$$

$$\sigma_x(y,t) = -\frac{\alpha E}{(1-v)}T(y,t)$$

where L is the diffusion length and κ the diffusivity, both are being assigned unit values.

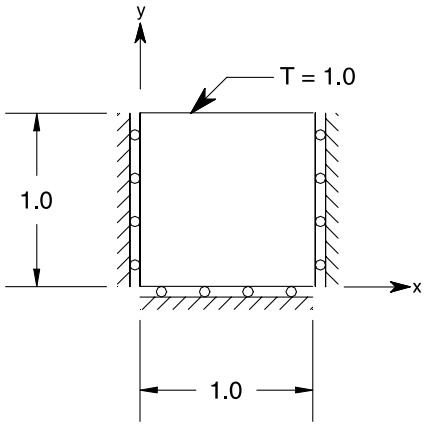

Fig. 1. A suddenly heated unit cube.

First the effect of aspect ratio is investigated for the present 2D and 3D particular integral formulations. The models are meshed in such a way that the number of elements in the diffusive (vertical) direction is set to 4 for all cases. The number of elements in the horizontal direction is set to 2 for $Lx = 0.25$ and 4 for other two cases of $Lx = 1.0$ and 4.0. The meshes for 2D and 3D are shown in Figs. 2 and 3. The computed values of temperature at $y = 0$, for a time step of 0.01, are shown in Figs. 4 and 5 for GSF1 and GSF2 for both 2D and 3D problems, together with their AS. Best solution is obtained for the $Lx = 0.25$ case. This can be expected because in such a geometry the GSFs can best represent the domain variation using the information available on the boundary. Generally for both 2D and 3D applications the solutions are extremely poor at early times, but improve as the steady state is approached. Although it is probably fair to state that for 3D these early time errors are only marginally tolerable. It can also be seen that the errors due to aspect ratio effect in all 3D cases are much less significant than those of the corresponding 2D solutions. The solutions for the displacement at $y = 1$ and the lateral stress $y = 0.5$ for a time step 0.01 are shown for the 3D problem in Figs. 6 and 7 respectively. These are once again better than the corresponding 2D results, but the results for GSF2 in 3D appear to be worse than those obtained for GSF1.

It is seen from Fig. 4(a) and (b) that there are some significant errors at the early times for the aspect ratio $Lx = 1.0$ even though the relatively large number of boundary elements (16 boundary elements) are used in this 2D analysis. In order to reduce these early time errors, effects of different GSFs, size of the time steps, use a Lagrange multiplier type constraints, etc. were investigated (see Park, 2001). It appears that the only way to reduce these errors in 2D is to include some interior points. Fig. 8(a) and (b) show the effect of

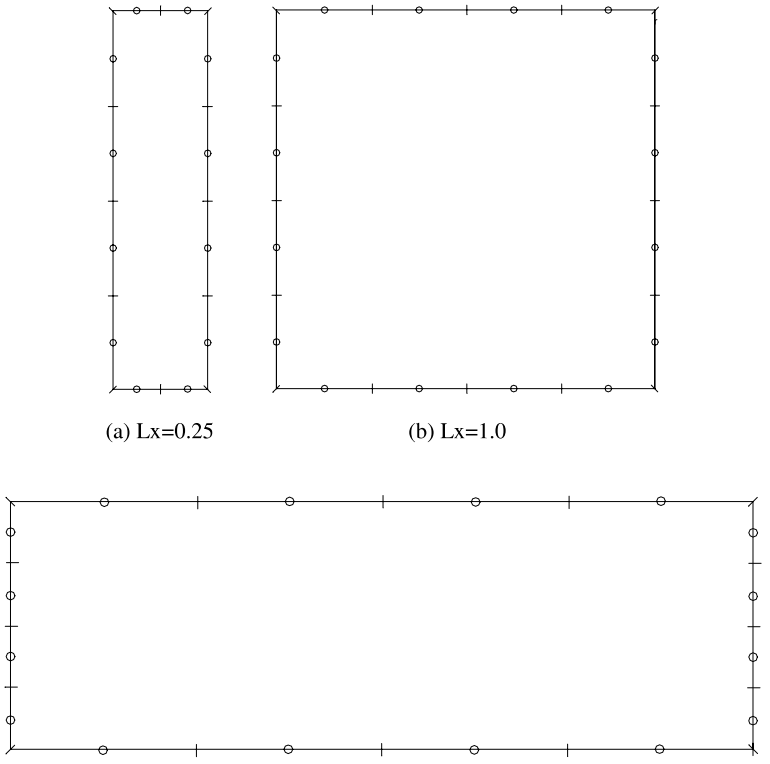

Fig. 2. Modeling mesh for aspect ratio effect (2D).

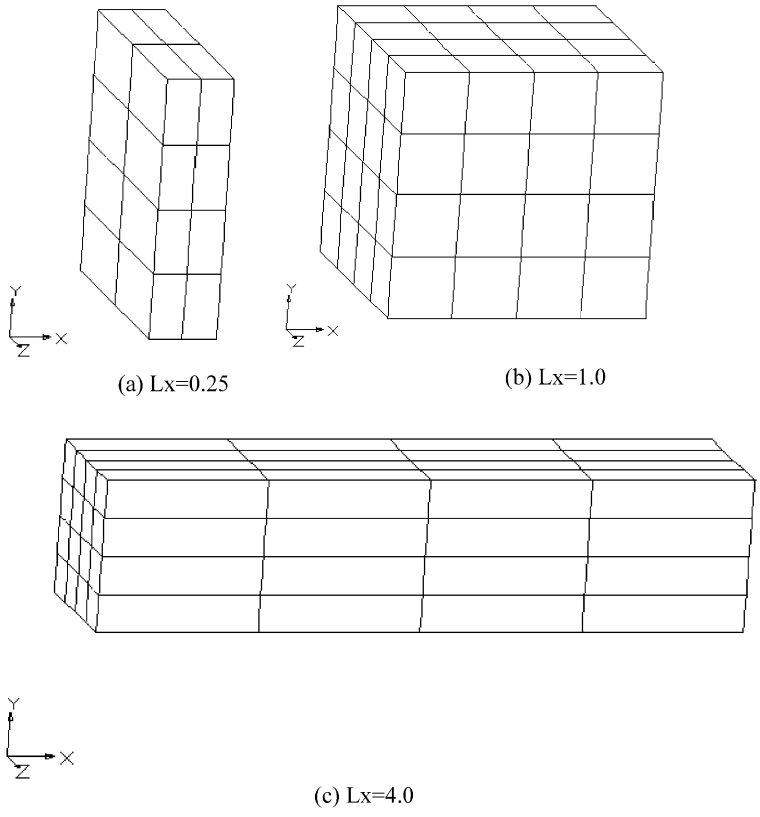

Fig. 3. Modeling mesh for aspect ratio effect (3D).

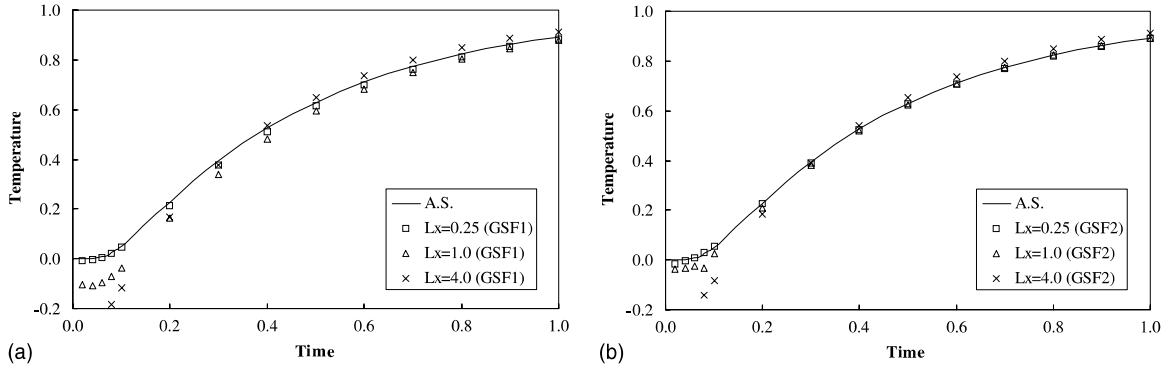

Fig. 4. (a) Effect of aspect ratio: temperature at $y = 0$ (GSF1, 2D). (b) Effect of aspect ratio: temperature at $y = 0$ (GSF2, 2D).

inclusion of interior points on results of temperature at $y = 0$. In these figures the number in the parenthesis represents the number of elements used for the analysis. Plus (+) sign indicates the additional number of the interior points involved. For example, (4) and (16) respectively represent 4 and 16 boundary elements, while

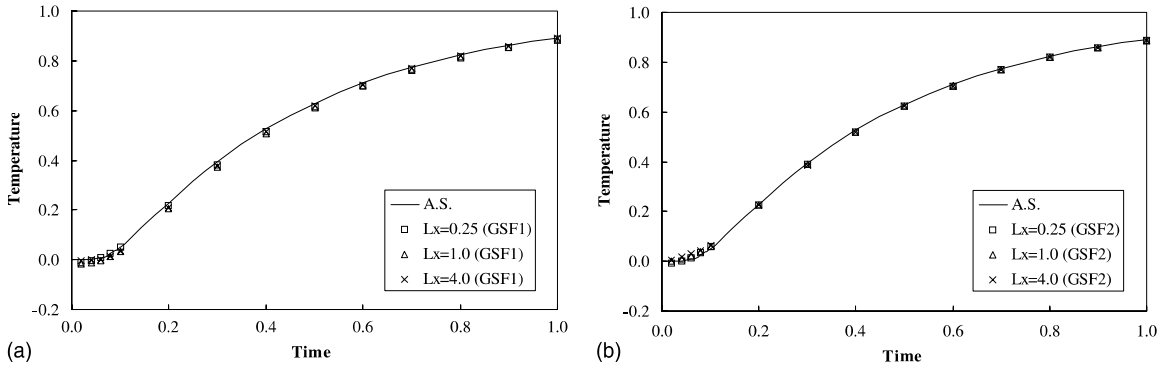

Fig. 5. (a) Effect of aspect ratio: temperature at $y = 0$ (GSF1, 3D). (b) Effect of aspect ratio: temperature at $y = 0$ (GSF2, 3D).

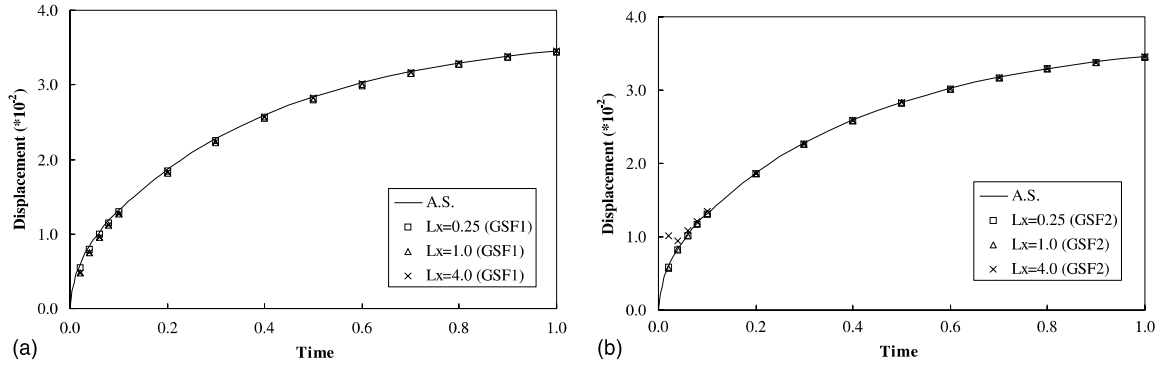

Fig. 6. (a) Effect of aspect ratio: displacement at $y = 1$ (GSF1, 3D). (b) Effect of aspect ratio: displacement at $y = 1$ (GSF2, 3D).

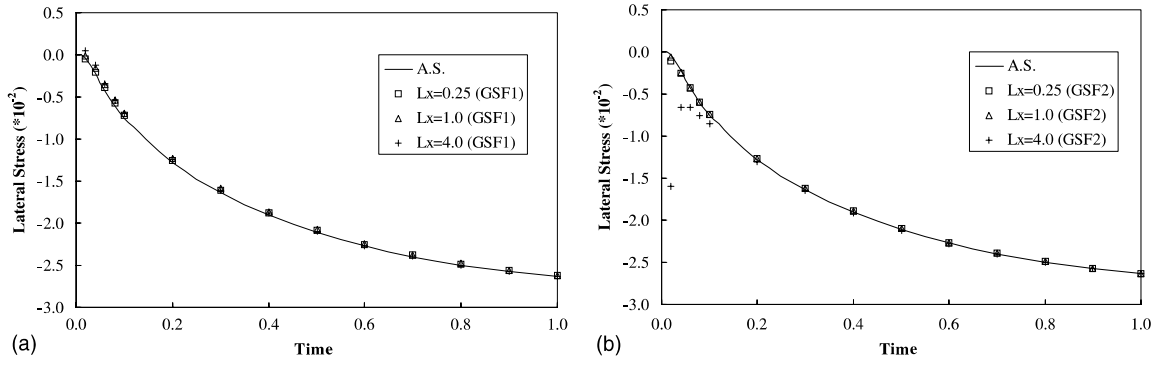

Fig. 7. (a) Effect of aspect ratio: lateral stress at $y = 0.5$ (GSF1, 3D). (b) Effect of aspect ratio: lateral stress at $y = 0.5$ (GSF2, 3D).

$(4 + 3)$ means 4 boundary elements and 3 interior points. It can be seen that with the introduction of even modest number of interior points (3 points), the results at the early time improve. Although not shown here, similar improvements are also visible in the displacement and stress results.

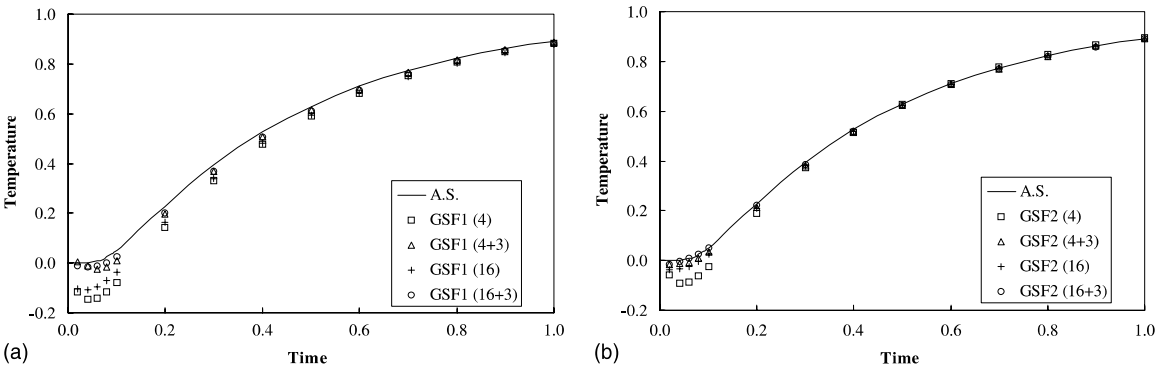

Fig. 8. (a) Effect of interior points: temperature at $y = 0$ (GSF1, 2D). (b) Effect of interior points: temperature at $y = 0$ (GSF2, 2D).

5.2. Example 2: a hollow cylinder

The second example is that of a hollow cylinder with initial temperature zero. The inner radius $a = 1$ and outer radius $b = 2$. The inner surface of the cylinder is maintained at a temperature of unity at time greater than zero, while the outer surface in maintained at temperature zero. In this case, only the positive octant of the cylinder is modeled, while symmetry constraints are imposed (Fig. 9). Fig. 10 shows typical 3D mesh with 48 quadratic boundary elements, where the front and back faces of the cylinder were assumed to be insulated roller boundaries.

The exact solutions of temperature T, displacement u and tangential stress σ_θ for this example problem can be obtained as (Carslaw and Jaeger, 1959, p. 207; Timoshenko and Goodier, 1951, p. 409)

$$T(r,t) = \frac{\ln\left(\frac{b}{r}\right)}{\ln\left(\frac{b}{a}\right)} T_{\mathrm{i}} + \pi \sum_{n=1}^{\infty} \frac{J_{\mathrm{o}}(b\alpha_n) J_{\mathrm{o}}(a\alpha_n)}{J_{\mathrm{o}}^2(a\alpha_n) - J_{\mathrm{o}}^2(b\alpha_n)} \{J_{\mathrm{o}}(r\alpha_n) Y_{\mathrm{o}}(b\alpha_n) - J_{\mathrm{o}}(b\alpha_n) Y_{\mathrm{o}}(r\alpha_n)\} \exp(-k\alpha_n^2 t)$$

$$u(r,t) = \frac{(1+v)\alpha}{(1-v)} \frac{1}{r} \int_a^r T(r,t) r \,\mathrm{d}r + H_1 r + \frac{H_2}{r}$$

$$\sigma_\theta(r,t) = \frac{\alpha E}{(1-v)} \frac{1}{r^2} \int_a^r T(r,t) r \,\mathrm{d}r - \frac{\alpha E}{(1-v)} T(r,t) + \frac{E}{(1+v)} \left(\frac{H_1}{1-2v} + \frac{H_2}{r^2} \right)$$

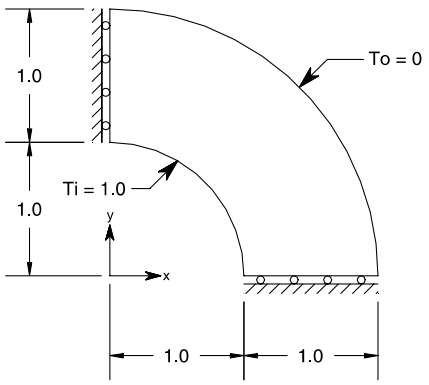

Fig. 9. A hollow cylinder.

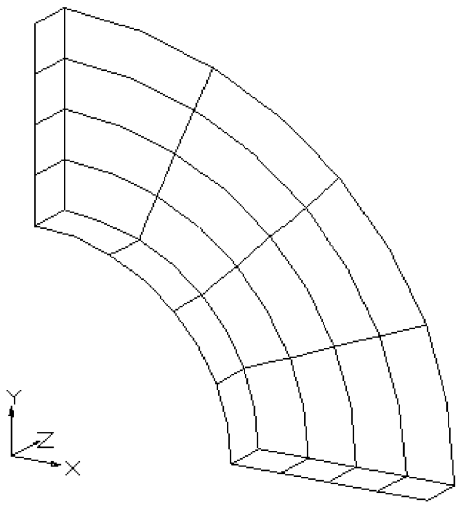

Fig. 10. Typical modeling mesh for a hollow cylinder.

where T_i is the constant temperature in the inner surface, J_o and Y_o are Bessel functions of the first and second kind respectively, α is the root of

$$J_o(a\alpha)Y_o(b\alpha) - J_o(b\alpha)Y_o(a\alpha) = 0,$$

and the constants H_1 and H_2 are

$$H_1 = \frac{(1-2\nu)\alpha(1+\nu)}{(1-\nu)} \frac{1}{(b^2-1)} \int_a^b T(r,t) r \, dr$$

$$H_2 = \frac{\alpha(1+\nu)}{(1-\nu)} \frac{1}{(b^2-1)} \int_a^b T(r,t) r \, dr$$

The results from the present formulation, for a time step of 0.01, are compared with the exact solutions in Figs. 11–15 for temperature at $r = 1.5$, and displacement and tangential stress at the inner and outer boundaries. For both of GSF1 and GSF2 good agreement can be obtained as the number of boundary

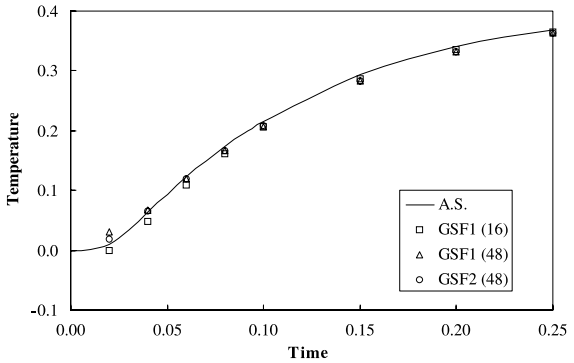

Fig. 11. A hollow cylinder: temperature at $r = 1.5$ (3D).

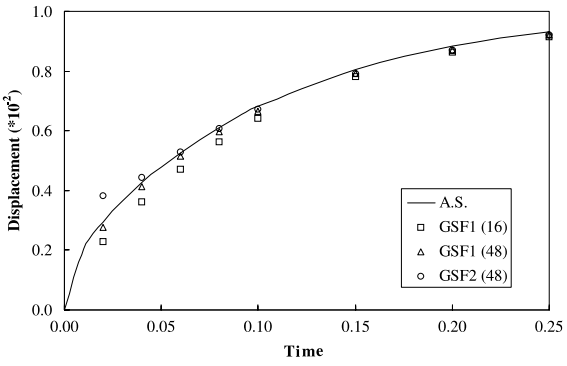

Fig. 12. A hollow cylinder: displacement at $r = 1$ (3D).

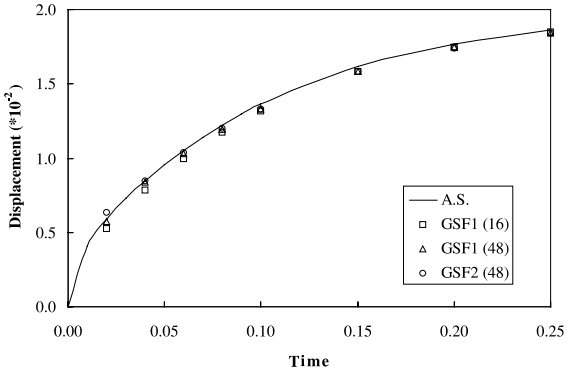

Fig. 13. A hollow cylinder: displacement at $r = 2$ (3D).

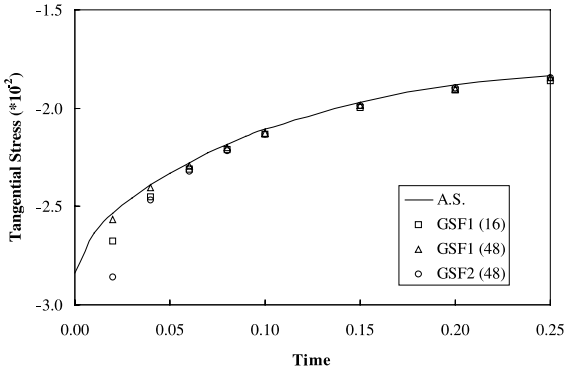

Fig. 14. A hollow cylinder: tangential stress at $r = 1$ (3D).

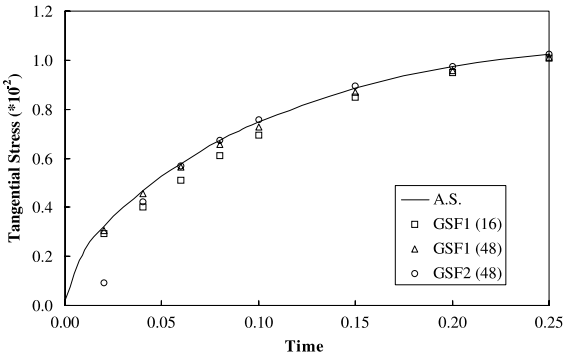

Fig. 15. A hollow cylinder: tangential stress at $r = 2$ (3D).

elements is increased from 16 to 48, except for the initial few values of tangential stress in GSF2 as shown in Figs. 14 and 15.

5.3. Example 3: a solid sphere

A solid sphere with a traction-free boundary and initial temperature zero is considered as the third example. The outer radius $a = 1$ is subjected to a sudden increase of temperature at time $t = 0$ and maintained at a temperature of unity. A quarter of sphere is analyzed (Fig. 16). Fig. 17 shows typical mesh with 48 quadratic boundary elements.

The exact solutions of temperature T, displacement u and tangential stress σ_θ for this example problem can be obtained as (Carslaw and Jaeger, 1959, p. 233; Timoshenko and Goodier, 1951, p. 417)

$$T(r,t) = T_o - 2T_o \sum_{n=1}^{\infty} (-1)^n \exp\left(-\frac{\kappa n^2 \pi^2 t}{a^2}\right)$$

$$u(r,t) = \frac{(1+\nu)\alpha}{(1-\nu)} \frac{1}{r^2} \int_0^r T(r,t) r^2 \, \mathrm{d}r + H_3 r + \frac{H_4}{r^2}$$

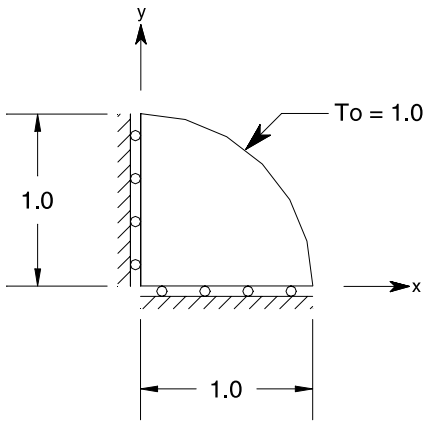

Fig. 16. A solid sphere.

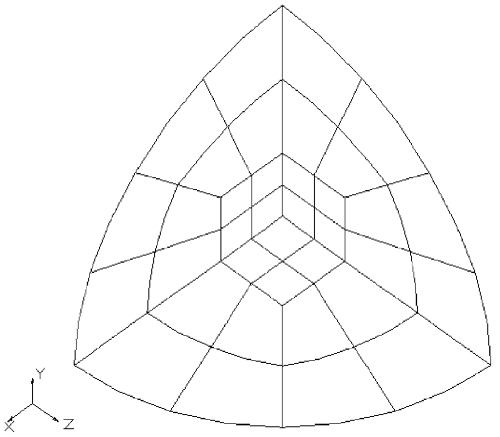

Fig. 17. Typical modeling mesh for a solid sphere.

$$\sigma_\theta(r,t) = \frac{\alpha E}{(1-\nu)}\frac{1}{r^3}\int_0^r T(r,t)r^2\,\mathrm{d}r - \frac{\alpha E}{(1-\nu)}T(r,t) + \frac{H_3}{1-2\nu} + \frac{E}{(1+\nu)}\frac{H_4}{r^3}$$

where T_o is the constant temperature at the outer surface, and the constants H_3 and H_4 are

$$H_3 = \frac{(1-2\nu)}{(1-\nu)}\frac{2\alpha}{a^3}\int_0^a T(r,t)r^2\,\mathrm{d}r$$

$$H_4 = 0$$

The results from the present formulations, for a time step of 0.01, are compared with the AS in Figs. 18–20 for temperature at the center, and displacement and tangential stress at the outer boundary. Again, good agreement can be obtained as the number of boundary elements is increased from 12 to 48, except for the initial few values of tangential stress in GSF2 as shown in Fig. 20. It is of considerable interest to note that these results would appear to converge without the aid of interior points.

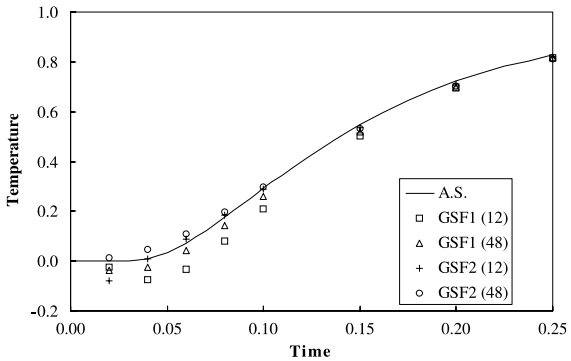

Fig. 18. A solid sphere: temperature at $r = 0$ (3D).

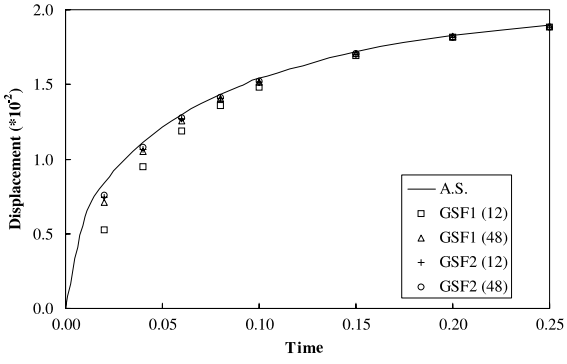

Fig. 19. A solid sphere: displacement at $r = 1$ (3D).

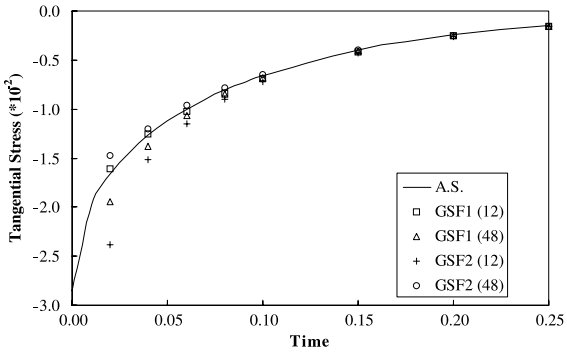

Fig. 20. A solid sphere: tangential stress at $r = 1$ (3D).

6. Conclusions

The particular integral formulations have been developed for the 2D and 3D transient uncoupled thermoelastic analysis. Unlike the previous formulations in the literature, the uncoupled thermoelasticity equation including the heat conduction equation was used to obtain the particular integrals. The equation of the steady-state thermoelasticity was used as the complementary function and two GSFs were chosen to approximate the transient term of the heat conduction equation. The present formulations were validated with three example problems.

The main conclusions of the present work are summarized in the following:

1. For the present particular integral formulations the effect of aspect ratio is investigated. $Lx = 0.25$ case gives better results in both 2D and 3D. However, in a 3D, the errors due to aspect ratio effect are less significant than those in a 2D problem.
2. To reduce the error at the early time, the effects of increase of the number of elements, inclusion of the interior points and the different choices of GSFs are considered. It appears that the only way to reduce the error at the early time in a 2D analysis is to include some of interior points. For a 3D analysis the error can be reduced by increasing the number of elements without using any interior points.
3. It appears that the particular integral method is a reasonably good alternative to the convolution method for 3D problems of transient uncoupled thermoelasticity.

Appendix A. Steady-state thermoelastic kernels

This appendix provides the details of all the kernel functions utilized in the steady-state uncoupled thermoelastic boundary element formulation of Eq. (20).

A.1. Two-dimensional kernels

For the displacement kernel,

$$G_{ij}(\mathbf{x},\xi)=\frac{1}{8\pi}\frac{1}{\mu(1-\nu)}\left[\frac{y_i y_j}{r^2}-\delta_{ij}(3-4\nu)\ln r\right] \tag{A.1}$$

$$G_{iT}(\mathbf{x},\xi)=\frac{1}{8\pi}\frac{(3\lambda+2\mu)\alpha}{k(\lambda+2\mu)}y_i r(1-2\ln r) \tag{A.2}$$

$$G_{TT}(\mathbf{x},\xi)=-\frac{1}{2\pi k}\ln r \tag{A.3}$$

whereas, for the traction kernel,

$$F_{ij}(\mathbf{x},\xi)=\frac{1}{4\pi}\frac{1}{(1-\nu)}\frac{1}{r}\left[-\frac{2y_i y_j y_\kappa n_\kappa}{r^3}-\frac{(\delta_{ij}y_\kappa n_\kappa+y_i n_j)}{r}(1-2\nu)+\frac{y_j n_i}{r}(1-2\nu)\right] \tag{A.4}$$

$$F_{iT}(\mathbf{x},\xi)=\frac{1}{8\pi}\frac{(3\lambda+2\mu)\alpha}{(\lambda+2\mu)}\left[\frac{2y_i y_\kappa n_\kappa}{r^2}-n_i(1-2\ln r)\right] \tag{A.5}$$

$$F_{TT}(\mathbf{x},\xi)=\frac{1}{2\pi r}\frac{y_\kappa n_\kappa}{r} \tag{A.6}$$

A.2. Three-dimensional kernels

For the displacement kernel,

$$G_{ij}(\mathbf{x},\xi)=\frac{1}{16\pi}\frac{1}{\mu(1-\nu)}\frac{1}{r}\left[\frac{y_i y_j}{r^2}+\delta_{ij}(3-4\nu)\right] \tag{A.7}$$

$$G_{iT}(\mathbf{x},\xi)=\frac{1}{8\pi}\frac{(3\lambda+2\mu)\alpha}{k(\lambda+2\mu)}\frac{y_i}{r} \tag{A.8}$$

$$G_{TT}(\mathbf{x},\xi)=\frac{1}{4\pi k}\frac{1}{r} \tag{A.9}$$

whereas, for the traction kernel,

$$F_{ij}(\mathbf{x},\xi)=\frac{1}{8\pi}\frac{1}{(1-\nu)}\frac{1}{r^2}\left[-\frac{3y_i y_j y_\kappa n_\kappa}{r^3}-\frac{(\delta_{ij}y_\kappa n_\kappa+y_i n_j)}{r}(1-2\nu)+\frac{y_j n_i}{r}(1-2\nu)\right] \tag{A.10}$$

$$F_{iT}(\mathbf{x},\xi)=\frac{1}{8\pi}\frac{(3\lambda+2\mu)\alpha}{(\lambda+2\mu)}\frac{1}{r}\left[\frac{y_i y_\kappa n_\kappa}{r^2}-n_i\right] \tag{A.11}$$

$$F_{TT}(\mathbf{x},\xi)=\frac{1}{4\pi r^2}\frac{y_\kappa n_\kappa}{r} \tag{A.12}$$

where v, the Poisson's ratio, x_i, coordinates of integration point, ξ_i, coordinates of field point, $y_i = x_i - \xi_i$, $r^2 = y_i y_i$.

Appendix B. Derivation of particular integrals

This Appendix contains the detailed derivation of particular integrals (u_i^{p}, t_i^{p}, T^{p} and q^{p}) for transient problems of uncoupled thermoelasticity by using the global shape function GSF1. The solutions for these particular integrals using the global shape function GSF2 essentially follow the same method of derivation.

B.1. Particular part

The particular part of the governing equation can be expressed from Eqs. (18) and (19) as

$$(\lambda+\mu)u^{\mathrm{p}}_{j,ji} + \mu u^{\mathrm{p}}_{i,jj} - (3\lambda+2\mu)\alpha T^{\mathrm{p}}_{,i} = 0 \tag{B.1}$$

$$kT^{\mathrm{p}}_{,jj} - \rho c_{\varepsilon}\dot{T} = 0 \tag{B.2}$$

B.2. Derivation of T^p and u_i^p

First T^{p} and u_i^{p} can be obtained as follows:
Let us assume that

$$\dot{T}(\mathbf{x}) = \sum_{n=1}^{\infty} C(\mathbf{x},\xi_n)\dot{\phi}(\xi_n) \tag{B.3}$$

$$T^{\mathrm{p}}(\mathbf{x}) = \sum_{n=1}^{\infty} D(\mathbf{x},\xi_n)\dot{\phi}(\xi_n) \tag{B.4}$$

$$u_i^{\mathrm{p}}(\mathbf{x}) = \sum_{n=1}^{\infty} U_i(\mathbf{x},\xi_n)\dot{\phi}(\xi_n) \tag{B.5}$$

where

$$C(\mathbf{x},\xi_n) = R - r \tag{B.6}$$

$$D(\mathbf{x},\xi_n) = (C_1 R - C_2 r)r^2 \tag{B.7}$$

$$U_i(\mathbf{x},\xi_n) = (D_1 R - D_2 r)r^2 y_i \tag{B.8}$$

By substituting (B.3)–(B.5) into (B.1) and (B.2), one can obtain the following equations

$$(\lambda+\mu)U_{j,ji} + \mu U_{i,jj} - (3\lambda+2\mu)\alpha D_{,i} = 0 \tag{B.9}$$

$$kD_{,jj} - \rho c_{\varepsilon} C = 0 \tag{B.10}$$

By substituting (B.6) and (B.7) into (B.10), the coefficients C_1 and C_2 can be derived

$$D_{,jj} = 2dC_1 R - 3(1+d)C_2 r \tag{B.11}$$

$$\therefore C_1 = \frac{\kappa}{2d}, \quad C_2 = \frac{\kappa}{3(1+d)} \tag{B.12}$$

In addition, by substituting (B.7) and (B.8) into (B.9), the coefficients D_1 and D_2 can be recovered to give

$$U_{j,ij} = U_{i,jj} = \{2(2+d)D_1R - 3(3+d)D_2r\}y_i \tag{B.13}$$

$$D_{,i} = (2C_1R - 3C_2r)y_i \tag{B.14}$$

$$\therefore D_1 = \frac{\beta C_1}{(2+d)}, \quad D_2 = \frac{\beta C_2}{(3+d)} \tag{B.15}$$

B.3. Derivation of t_i^p

Next t_i^{p} can be derived as follows:
Let us assume that σ_i^{p} can be expressed as

$$\sigma_{ij}^{\mathrm{p}}(\mathbf{x}) = \sum_{n=1}^{\infty} S_{ij}(\mathbf{x}, \xi_n)\dot{\phi}(\xi_n) \tag{B.16}$$

Considering the strain–displacement relation and the stress–strain law:

$$\sigma_{ij}^{\mathrm{p}}(\mathbf{x}) = \delta_{ij}\lambda\varepsilon_{ll}^{\mathrm{p}}(\mathbf{x}) + 2\mu\varepsilon_{ij}^{\mathrm{p}}(\mathbf{x}) - \delta_{ij}(3\lambda + 2\mu)\alpha T^{\mathrm{p}}(\mathbf{x}) \tag{B.17}$$

or

$$S_{ij}(\mathbf{x}, \xi_n) = \delta_{ij}\lambda E_{ll}(\mathbf{x}, \xi_n) + 2\mu E_{ij}(\mathbf{x}, \xi_n) - \delta_{ij}(3\lambda + 2\mu)\alpha D(\mathbf{x}, \xi_n) \tag{B.18}$$

where

$$E_{ll} = \frac{\partial U_l}{\partial x_l} = \{(2+d)D_1R - (3+d)D_2r\}r^2 \tag{B.19}$$

$$E_{ij} = \frac{1}{2}\left(\frac{\partial U_i}{\partial x_j} + \frac{\partial U_j}{\partial x_i}\right) = (D_1R - D_2r)r^2\delta_{ij} + (2D_1R - 3D_2r)y_iy_j \tag{B.20}$$

Then t_i^{p} can be obtained by considering the appropriate normals as

$$t_i^{\mathrm{p}}(\mathbf{x}) = \sum_{n=1}^{\infty} H_i(\mathbf{x}, \xi_n)\dot{\phi}(\xi_n) \tag{B.21}$$

where

$$H_i(\mathbf{x}, \xi_n) = S_{ij}(\mathbf{x}, \xi_n)n_j(\mathbf{x}) \tag{B.22}$$

B.4. Derivation of q^p

Finally q^{p} can be derived from Eq. (B.4) as

$$q^{\mathrm{p}}(\mathbf{x}) = \sum_{n=1}^{\infty} Q(\mathbf{x}, \xi_n)\dot{\phi}(\xi_n) \tag{B.23}$$

where

$$Q(\mathbf{x}, \xi_n) = -k\frac{\partial D}{\partial n} = -k(2C_1R - 3C_2r)y_in_i \tag{B.24}$$

References

Banerjee, P.K., 1994. The Boundary Element Methods in Engineering. McGraw-Hill, London.

Banerjee, P.K., Butterfield, R., 1981. Boundary Element Methods in Engineering Science. McGraw-Hill, London.

Carslaw, H.S., Jaeger, J.C., 1959. Conduction of Heat in Solids. Clarendon Press, Oxford.

Chopra, M.B., 1992. Linear and nonlinear analysis of axisymmetric problems in thermomechanics and soil consolidation. Ph.D. Dissertation. State University of New York at Buffalo, Buffalo, New York.

Dargush, G.F., 1987. Boundary element methods for the analogous problems of thermomechanics and soil consolidation. Ph.D. Dissertation. State University of New York at Buffalo, Buffalo, New York.

Dargush, G.F., Banerjee, P.K., 1989. Development of a boundary element method for time-dependent planar thermoelasticity. Int. J. Solids Struct. 25, 999–1021.

Dargush, G.F., Banerjee, P.K., 1990. BEM analysis for three-dimensional problems of transient thermoelasticity. Int. J. Solids Struct. 26, 199–216.

Dargush, G.F., Banerjee, P.K., 1991a. A new boundary element method for three-dimensional coupled problems of consolidation and thermoelasticity. J. Appl. Mech. ASME 58, 28–36.

Dargush, G.F., Banerjee, P.K., 1991b. Boundary element methods for three-dimensional thermoplasticity. Int. J. Solids Struct. 27, 549–565.

Dargush, G.F., Banerjee, P.K., 1992. Time dependent axisymmetric thermoelastic boundary element analysis. Int. J. Numer. Meth. Eng. 33, 695–717.

Deb, A., Banerjee, P.K., 1991. Multi-domain two- and three-dimensional thermoelastic analysis by BEM. Int. J. Numer. Meth. Eng. 32, 991–1008.

Deb, A., Henry Jr., D.P., Wilson, R.B., 1991. An alternative BEM for 2D and 3D anisotropic thermoelasticity. Int. J. Solids Struct. 27, 1721–1738.

Henry Jr., D.P., Banerjee, P.K., 1988. A new boundary element formulation for two- and three-dimensional thermoelasticity using particular integrals. Int. J. Numer. Meth. Eng. 26, 2061–2078.

Raveendra, S.T., 2000. The use of a piecewise continuous polynomial basis function for the surface reduction of integral equations in thermoelastic analysis. Comp. Struct. 77, 601–604.

Park, K.H., 2001. Development of BEM for transient coupled problems, Ph.D. Dissertation, State University of New York at Buffalo, February 2001.

Rizzo, F.J., Shippy, D.I., 1977. An advanced boundary integral equation for three-dimensional thermoelasticity. Int. J. Numer. Meth. Eng. 11, 1753–1768.

Timoshenko, S.P., Goodier, J.N., 1951. Theory of Elasticity. McGraw-Hill, New York.

Wang, C.B., 1995. Advanced development of boundary element method in material nonlinear analysis. Ph.D. Dissertation. State University of New York at Buffalo, Buffalo, New York.

Wang, H.C., Banerjee, P.K., 1988. Axisymmetric free vibration problems by the boundary element method. J. Appl. Mech. ASME 55, 437–442.